

Applications of Image Recognition for Real-Time Water Level and Surface Velocity

Franco Lin, Wen-Yi Chang, Lung-Cheng Lee, and
Hung-Ta Hsiao, Whey-fone Tsai
National Center for High-Performance Computing
National Applied Research Laboratories
Tainan, Taiwan
{n00fli00,c00wyc00,lclee,c0074300,c00wft00}@nchc.
org.tw

Jihn-Sung Lai
Hydrotech Research Institute
National Taiwan University
Taipei, Taiwan
jslai525@ntu.edu.tw

Abstract—In this paper, we present two types of the real-time water monitoring system using the image processing technology, the water level recognition and the surface velocity recognition. According to the bridge failure investigation, floods in the river often pose potential risk to bridges, and scouring could undermine the pier foundation and cause the structures to collapse. It is very important to develop monitoring techniques for bridge safety in the field. In this study, we installed two high-resolution cameras on the in-situ bridge site to get the real-time water level and surface velocity image. For the water level recognition, we use the image processing techniques of the image binarization, character recognition, and water line detection. For the surface velocity recognition, the proposed system apply the PIV(Particle Image Velocimetry, PIV) method to obtain the recognition of the water surface velocity by the cross correlation analysis. Finally, the proposed systems are used to record and measure the variations of the water level and surface velocity for a period of three days. The good results show that the proposed systems have potential to provide real-time information of water level and surface velocity during flood periods.

Keywords- water level; monitoring; image process; velocity;

I. INTRODUCTION

In the age of severe climate change, torrential rainfall and flooding often cause bridges destroyed or collapsed. These events will seriously affect the lives of people and homeland security. Therefore, it's very crucial to real-time monitor the flow situation during the high flow, better with the non-contact and automatic measurement techniques. In the past 20 years, the flow visibility and image processing technology has been applied. Essentially, image processing can replace the human eye with the implementation of the visualization decision, and avoid expensive human resources. Compared to other non-contact methods, such as the microwave radar, image-based methods may cost less human resources and money, but still have advantages of automation, convenience, and efficiency. Fujita et al. (1998)[1] applied PIV (Particle Image Velocimetry, PIV) method to obtain the surface velocity of the flood. Weitbrecht et al. (2002)[2] used the PIV method to observe surface velocity changes in the shallow water wave. Muste et al. (2004)[3] used PIV method in the hydraulic

experiments. Kim et al. (2008)[4] developed the mobile LSPIV (large-scale PIV), which can be deployed in the fields quickly. Hauet et al. (2008)[5] established the real-time LSPIV system, and monitored the river flow in five months. Compared to the data measured by the U.S. Geological Survey, the measurement error is about 10%. In the above literature review, it shows feasible to use the PIV system for real-time measurements in the flood.

In order to obtain real-time monitoring image, as in Figure 1(a), two high-resolution monitoring cameras were set up at the in-situ measurement sites. One camera was set up on the side of the bridge, top-viewing the river surface, and it is used for recognizing the river surface velocity. In Figure 1(b), the other camera was set up to capture the water gauge, which is used to get the water level of Feitsui reservoir. In order to provide sufficient light at night, and he IR spotlight was also set up in the field. Also, in order to avoid rain to affect the image quality, the wiper was installed outside the windshield of the camera. The monitoring images of cameras were transmitted to the local server through the network, and then were image processed in real-time.



Figure 1. Measurement sites

II. WATER LEVEL IMAGE RECOGNITION

This section presents an image processing method to recognize the water level in Feitsui reservoir. Figure 2 is the flowchart for recognition of the water level. First, the high-resolution camera beside the dam can capture images with the water gauge and water line. Second, we can interpolate the water level according to the detection of the water line and water gauge.

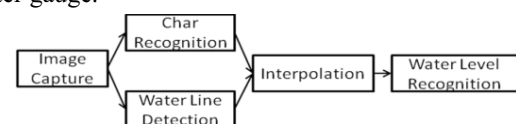


Figure 2. Flowchart to recognize the water level

A. Detect the Water Line By Thresholding

There may be many ways to recognize the water line, however, some of them may not be suitable for detecting the water line under the field conditions. For instance, we tried to measure the water line by detecting the uneven luminance; but because of the reflection of ruler on the water surface which also generates the uneven luminance, and the threshold value can't be found appropriately; In addition, we also tried to use motion detection method to split the foreground and background; but due to the shake of camera during the typhoon periods, the method is not suitable for this environment. Finally, we used the edge detection method to identify the water line between the edge of the water line and water gauge. We employed the feature that the water gauge is not visible under the water, and the body of the water gauge above the water surface can be detected by the edge detection method. Once the body of the ruler above the water is recognized, the bottom edge line can represent the water line. The following is the recognition process of the water line. From the flowchart of Figure 3, this process is divided into two parts; the first part is the character recognition, and the other part is the search of the water line. Figure 3 shows the recognition process for the water line search algorithm, which includes the following algorithm steps:

- 1) *Gray image*
- 2) *Histogram equalization*
- 3) *Threshold using Otsu method*
- 4) *Remove small object and use Morphology*

Figure 3 (a) ~ (d) are the results of each stage of the algorithm. Figure 3 (e) is the recognition result of the water line, designated as a red line. In this study, we simply use the bottom-up approach to get the water line from the lower bound of the ruler body.

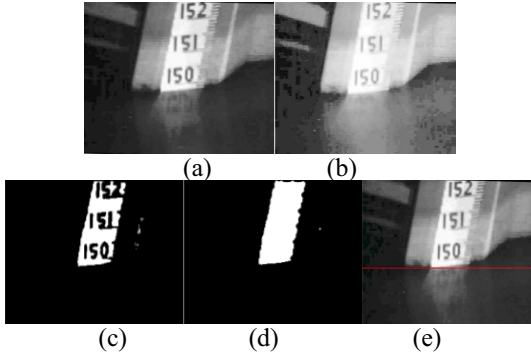


Figure 3.(a) Gray (b) H.Q.(c) Binary (d) Morphology (e) The water line

B. Recognite the Char on Bridge

In the previous section, the algorithm can recognize the water line, but you still don't know the actual water height. So, if we can recognize water gauge characters, then we can calculate the actual water level according to the positions of water line and characters. The following process is the algorithm of the character recognition, also shown in Figure 4:

- 1) *The vertical direction of the median filter smooth horizontal scale line in grayscale images*

- 2) *Get the characters form Bottom-hat filter*
- 3) *Thresholding from Otsu*
- 4) *Remove small object and non-character properties(The height of the object must be greater than the width)*

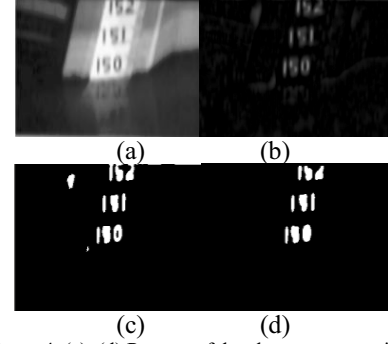


Figure 4. (a)~(d) Process of the character recognition

Then, we need to decompose characters. From Figure 4 (d), we can get character range from horizontal and vertical projection. One can separate each character range from gray images. In Figure 5, we can extract a clear number image by Otsu method[6], for instance, we can get a complete character, "151".

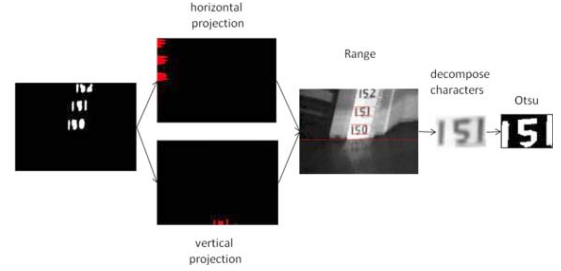


Figure 5. Decompose characters

In Figure 6, the character image by Otsu method may contain some noises. The horizontal noise is due to the water gauge scale, not the characters, so non-characters noise may be filtered by the rule, $height > width / 3$.



Figure 6. Noise and non-noise image

In Figure 6, the number can be further separated into three characters, respectively. By using the template match method, we can match this character with the template character according to the template match function, which gives a minimum score when matching. Eq. (1) is the template match equation of the image f and w , and M, N are the template size.

$$c(s, t) = \sum_x \sum_y f(x, y) w(x - s, y - t) \quad (1)$$

$$s = 0, 1, 2, \dots, M - 1, t = 0, 1, 2, \dots, N - 1$$

After the recognition of character and water line, we can use interpolation method to calculate the actual height of the water line. As the arrows in Figure 7, two sets of characters

are recognized at least for each water image. Taking the lower edge of the character as a reference line, the water level is obtained using the linear interpolation method.

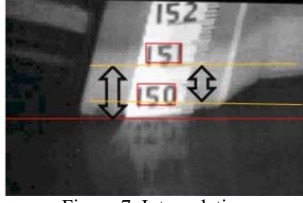


Figure 7. Interpolation

III. SURFACE VELOCITY RECOGNITION

The flow velocity in rivers plays a very important role in water resource management and hazard mitigation, such as inundation prevention, bridge safety evaluation, reservoir operation, etc., which all needs the information of river flow during floods. Most of traditional flow measurement tools, such as Propeller Velometer and Electro-Magnetic Current Meter, are contacting river velocity measurements, and they are difficult to use during the typhoons and floods. Figure 8 shows Propeller Velometer and Electro-magnetic Current Meter.



Figure 8. Propeller Velometer and Radio Current Meter

The non-contacting flow velocity measurements are mainly the image measurement method and the microwave radar method, such as Acoustic Doppler Velocimeter. The concept of image measurement method is based on tracking the particle displacement to calculate the surface velocity. The typical method is Particle Image Velocimetry (Willert et al (1991)[7], having the capacity of the wide range of measurement.

In recent years, PIV is one of the popular tools for a wide range of flow field monitoring. In this study, we also conducted the recognition of surface velocity using PIV technology. The flowchart of image processes for the flow velocity monitoring system is shown in Figure 9.

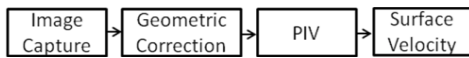


Figure 9. Flowchart of PIV method

A. Geometric Correction

First, the camera can capture the high-resolution image, and then the perspective of the camera is corrected by a geometric correction. Eq. (2) shows the corresponding relationship between the two systems, which is known as DLT (Direct Linear Transformation) equation. According to Eq. (2), at least six control points are needed to solve the equation coefficients, and the actual water level Z_0 may be

obtained by the recognition of the water level in the previous chapter, L_0 - L_{11} are the parameters of the transformation.

$$\begin{cases} x = \frac{L_1 X_o + L_2 Y_o + L_3 Z_o + L_4}{L_9 X_o + L_{10} Y_o + L_{11} Z_o + 1} \\ y = \frac{L_5 X_o + L_6 Y_o + L_7 Z_o + L_8}{L_9 X_o + L_{10} Y_o + L_{11} Z_o + 1} \end{cases} \quad (2)$$

B. Particle image velocimetry Method

The traditional PIV algorithm (Adrian, 1991)[8] for the surface velocity is to analyze the correlation of the consecutive images. A fixed-size window (Interrogation Area, IA) is selected in the First image, and the same position of the window in the second image is also chosen for calculating the correlation. In the present study, the correlation is obtained by matching the cross-correlation coefficient (Cross-Correlation Coefficient), which can be calculated by the following relationship, Eq. (3):

$$\phi_{fg}(m, n) = \sum_{x=1}^M \sum_{y=1}^N f(x, y) g(x+m, y+n) \quad (3)$$

in which $f(x, y)$ is the pixel value of the coordinates (x, y) at time t , and $g(x, y)$ is the pixel value at time $t+1$. M and N are the size of IA windows, and m and n are movement index. In the present study, the origin image size is 1280×960 , and IA size is 32×32 . Obtaining the maximum value $\phi_{fg}(\hat{m}, \hat{n})$ at time t , the pixel value of IA movement are \hat{m} and \hat{n} .

Eq. (3) represents the calculation of cross-correlation coefficient in the spatial domain. In order to improve the calculation efficiency, Eq. (3) can be transformed into the frequency domain by a fast Fourier transform and shown as Eq. (4). In the equation, the original $f(x, y)$ and $g(x, y)$ in the spatial domain can be converted to $F(u, v)$ and $G(u, v)$ in the frequency domain, and F^* is the complex conjugate of $F(u, v)$.

$$\begin{aligned} f(x, y) &\leftrightarrow F(u, v) \\ g(x, y) &\leftrightarrow G(u, v) \\ \phi_{FG}(u, v) &= F^*(u, v) G(u, v) \end{aligned} \quad (4)$$

Figure 10 is a cross-correlation coefficient map by analyzing two consecutive image blocks. In the figure, the detected peak of this image represents the most possible position of particle movement. If the peak point remains at the central point of the image, it means flow particles have no displacement. If the peak point leaves from the center, it indicates the flow particles move from the center to the peak. Dividing the displacement by the time increment, the flow vector can be obtained.

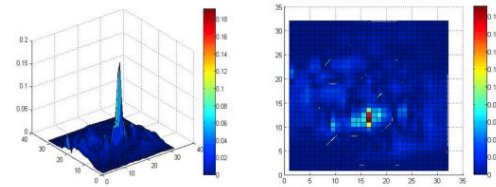


Figure 10. Cross-correlation coefficient map

In the above method, the calculation of particle displacement has the accuracy of one pixel. In fact, as shown in Figure 10, the peak value may not occur exactly at the grid point. In order to improve the accuracy to the subpixel level, a quadratic curve method is proposed. In this study, we used the quadratic curve $y = Ax^2 + Bx + C$ to fit the correlation value to obtain the real peak position, as shown in Figure 11.

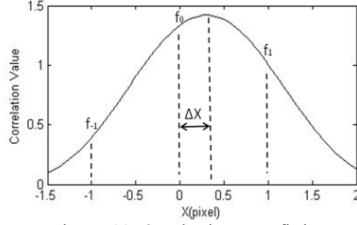


Figure 11. Quadratic curve fitting

In the figure, 3 correlation values can be used to determine the coefficients of the quadratic curve, and the position of the real peak can be obtained by making the differential equation equal 0. Thus, the displacement of the actual subpixel ΔX in the three-point relationship can be obtained as Eq. (5):

$$\Delta X = \frac{f_1 - f_{-1}}{2(f_0 - f_{-1} - f_1)} \quad (5)$$

IV. EXPERIMENTS AND CONCLUSIONS

Figure 12 is the recognized surface velocity image. Green line region is the domain of interest. Figure 12 (a) displayed the recognition results during the day. In the figure, the flow direction is from the northeast to the southwest, and the velocity is slower near stones. At night, in Figure 12(b), IR LED Camera can increase the luminance; therefore, the flow vectors are still recognized. Figure 13 shows the velocity variations in three days. The three-day average flow velocity is approximately 0.75 m/s, and the maximum variation from the average is about 0.4 m/s.

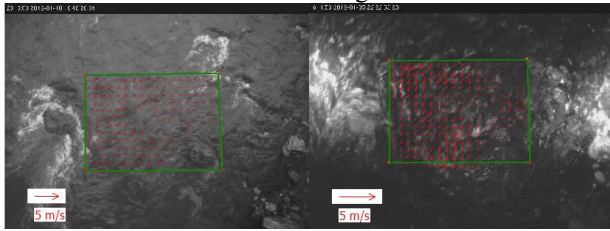


Figure 12. Flow velocity at (a) day (b) night

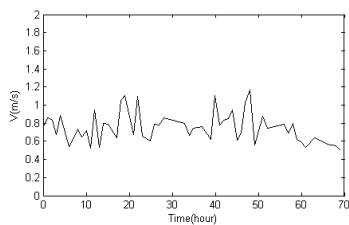


Figure 13. Surface velocity in 3 days

For the water level recognition, the image data captured by the camera at Feitsui reservoir are analyzed for a period

of 3 days. In Figure 14 the horizontal axis is time, and the vertical axis is the water level. One can see that the water level is gradually reduced in this period. Generally, the recognition water levels agree well with the measured data. From the experimental results, the water level recognition method developed in this study can automatically and accurately recognize the water level in Feitsui Reservoir. Thus the long-term water-level recognition would be feasible in the future.

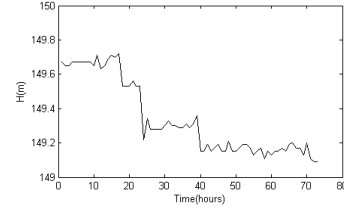


Figure 14. Water level recognition in 3 days

In this study, we develop the real-time water level and surface velocity recognition system. Two high-resolution cameras are used to acquire the image data, and the proposed methods can successfully real-time monitor the river water level and surface velocity data. To overcome in-situ problems, the IR spotlight device is effective at night, and the movement detection method is useful to the camera vibration. In the future, we will extend our systems to the other rivers for a long-term recording and systematic monitoring of river systems.

ACKNOWLEDGMENT

Financial support from the National Science Council, Taiwan, under grant NSC 101-2625-M-492-006 is highly appreciated. We are also grateful to the National Center for High-Performance Computing for computer time and facilities.

REFERENCES

- [1] Fujita I, Muste M. and Kruger A., "Large-scale particle image velocimetry for flow analysis in hydraulic applications", *J. Hydraul. Res.*, Vol. 36, No. 3, (1998), pp 397-414.
- [2] Weitbrecht V., Kuhn G. and Jirka G. H., "Large scale PIV-measurement at the surface of shallow flows", *Flow. Meas. Instrum.*, Vol. 13, (2002), pp 237-245.
- [3] Muste M., Xiong Z., Schone J. and Li Z., "Flow diagnostic in hydraulic modeling using image velocimetry", *J. Hydrol. Eng.*, Vol. 130, No. 3, (2004), pp 175-185.
- [4] Kim Y., Muste M., Hauet A., Krajewski W. F., Kruger A. and Bradley A., "Stream discharge using mobile large-scale particle image velocimetry: A proof of concept," *Water Resour. Res.*, Vol. 44, (2008), W09502, doi:10.1029/2006WR005441.
- [5] Hauet A., Kruger A., Krajewski W., Bradley A., Muste M., Creutin J.-D. and Wilson M., "Experimental system for real-time discharge estimation using an image-based method," *J. Hydrol. Eng.*, Vol. 13, No. 2, (2008), pp 105-110.
- [6] Otsu, N., "A Threshold Selection Method from Gray-Level Histograms," *IEEE Transactions on Systems, Man, and Cybernetics*, Vol. 9, No. 1, 1979, pp. 62-66.
- [7] Willert, C. E. and M. Gharib, "Digital particle image velocimetry," *Exp. Fluids* 10,p.181-193 (1991)
- [8] Adrian, R. J., "Particle-imaging techniques for experimental fluid mechanics," *Annu. Rev. Fluid Mech.*, Vo. 23, (1991), pp261- 304.